Mecánica Computacional Vol. XXI, pp. 1675–1692
S. R. Idelsohn, V. E. Sonzogni and A. Cardona (Eds.)
Santa Fe–Paraná, Argentina, October 2002

GEOMETRICALLY NONLINEAR STRUCTURAL ANALYSIS USING THE EIGHT-NODE HEXAHEDRAL ELEMENT WITH ONE-POINT QUADRATURE AND HOURGLASS CONTROL

Luiz A. Duarte Filho[*] and Armando M. Awruch[†]

[*] Centro de Mecânica Aplicada e Computacional (CEMACOM)
Universidade Federal do Rio Grande do Sul
Osvaldo Aranha, 99, centro
90035-160 Porto Alegre, Brasil
e-mail: duarte@cttmar.univali.br

[†] Centro de Mecânica Aplicada e Computacional (CEMACOM)
Universidade Federal do Rio Grande do Sul
Osvaldo Aranha, 99, centro
90035-160 Porto Alegre, Brasil
e-mail: awruch@adufrgs.ufrgs.br

Key words: Geometrically Nonlinear Analysis, Finite Elements, Reduced Integration, Hourglass Control, Corotational Formulation.

Abstract. *An eight-node hexahedral element with uniform reduced integration, which is free of volumetric and shear locking and has no spurious singular modes, is implemented here for geometrically nonlinear static structural analysis. In the element formulation, one-point quadrature is used so that the element tangent stiffness matrix is given explicitly and computational time is substantially reduced in the geometrically nonlinear analysis. In order to avoid shear locking the generalized strain vector is written in a local corotational system and certain non-constant terms in the shear strain components are omitted. The volumetric locking is cured by setting the dilatational part of the normal strain components to be constant. A corotational procedure is employed to obtain the deformation part of the displacement increment in the corotational system and update element stresses and internal force vectors. Numerical examples verify the computational efficiency and the potential of the three-dimensional element in the analysis of shells, plates and beams undergoing large displacements and rotations. Results are compared to those employing classical plate and shell elements.*

1 INTRODUCTION

The development of reliable and efficient elements for nonlinear analysis of plates and shells is one of the most challenging topics in finite element research today. Basically, there are three major thrusts of element technology in continuum elements: to obtain elements with better performance for large-scale calculations; to avoid locking for thin structures and to eliminate the difficulties associated with the treatment of incompressible materials.

For large-scale calculations, element technology has focus on underintegration to achieve faster elements, which are specially important for geometrically nonlinear analysis and explicit dynamic schemes. For three dimensions, cost reductions on the order of 8 have been achieved through underintegration compared to full integration [1]. Therefore, one point quadrature elements are extensively used in modern codes, in which the element tangent stiffness matrix is given explicitly. However, the results from one-point quadrature elements may be meaningless if spurious modes are excited so that, an efficient stabilization of the element is required.

Within recent years, a great understanding of the subject has been achieved in the literature, specially in papers due to Belytschko, Liu and co-workers. Many techniques have been proved successful, but some of them have their limitation.

In earlier papers, Belytschko *et al*. [2-3] developed the one-point quadrature elements with hourglass control provided by introducing an "artificial damping" or "artificial stiffness". In these works, the magnitude of the stabilization terms is controlled by a user input stabilization parameter.

An alternative approach in which the resulting stabilization matrix requires no user-specified parameters was proposed by Liu *et al*.[4]. It is shown that the stabilization vector γ can be obtained simply by taking the partial derivatives of the general strain vector with respect to the natural coordinates. The strain vector is approximated by the combination of a constant part and other parts involving strain derivatives. However, shear-related locking phenomena are not taken into consideration so that they are not suitable for bending analysis. Besides, no three-dimensional results is reported in their study. Schulz [5] establishes a hourglass control procedure by expanding the stress in a Taylor series about the element center. It is found that the hourglass modes are suppressed by the retention of the first and the second derivative terms in the expansion. However, only two dimensional problems are reported.

Liu *et al*.[6] also developed an underintegrated eight-node hexahedral element based on the procedures given in Liu *et al*.[4]. In order to avoid shear locking, the generalized strain vector is written in a local corotational system and certain non-constant terms in the shear strain components are omitted. The volumetric locking is cured by setting the dilatational part of the normal strain components to be constant. To improve accuracy over one-point quadrature elements, several quadrature points are used to integrate the internal forces, specially for plastic problems. It has been shown that these elements provide good results in thin shell bending and sheet metal forming analysis. However, due to the special setting of four-point quadrature, the brick elements are "frame dependent" and are also expensive compared to one-point quadrature elements [7].

Based on the multiple-quadrature formulation given in Liu *et al*.[6] a Hu and Nagy [7] proposed a new simple one-point quadrature hexahedral element. The strain and stress vectors are firstly expanded in a Taylor series at the element center up to bilinear terms. The constant terms are used to compute the element internal force vector and the linear and bilinear terms are used to form the hourglass resisting force vector. As shown in Liu *et al*.[6], the corotational system is employed to remove those modes associated with shear locking and the dilatational part of gradient matrix is evaluated only at the center of the element to avoid volumetric locking. In this paper, the performance of the element is verified only for linear static and dynamic analysis.

Recently, Liu *et al*.[8] implemented the multiple-quadrature element described in Liu *et al*.[6] for large deformation elastoplastic analysis. As in the multiple-quadrature formulation the elimination of the shear locking depends on the proper treatment of the shear strain in the local coordinate system, the finite element formulation for large deformation are derived in the corotational coordinate system.

In this work, the eight-node hexahedral element proposed by Hu and Nagy [7] is implemented and tested for geometrically nonlinear analysis. The formulation for nonlinear analysis described in Liu *et al*.[8] is employed here for the particular case of small strain/large rotation.

Thus, the objective of this work is to verify the computational efficiency and the robustness of the eight-node hexahedral element with one-point quadrature developed by Hu and Nagy [7] in the analysis of shells, plates and beams undergoing large displacements and rotations. The numerical examples presented here demonstrate that is possible to solve the critical problems for geometrically nonlinear analysis of shells with three-dimensional element.

It is well known that there are many new plate/shell elements which are free of shear and membrane locking and have been applied successfully to thin shell analysis [9-11]. However, they may not be suitable for some engineering aplication (3D structures, for instance).

2 PRINCIPLE OF VIRTUAL WORK

In a finite element representation, the principle of virtual work is given by:

$$\delta \mathbf{W}_e^{\text{int}} = \int_{V_e} \delta \mathbf{u}^t \mathbf{b} \, \mathrm{d}V + \int_{S_e} \delta \mathbf{u}^t \overline{\mathbf{p}} \, \mathrm{d}S \,, \tag{1}$$

where the superscript t designates the transpose; $\delta\mathbf{u}$ is the virtual displacement vector in the element "e"; $\mathbf{b}$ is the body force vector applied in V_e; $\overline{\mathbf{p}}$ is the traction vector applied on S_e; $\mathbf{W}_e^{\text{int}}$ is the element internal virtual work given by:

$$\delta \mathbf{W}_e^{\text{int}} = \int_{V_e} \delta \varepsilon^t \sigma \, \mathrm{dV} \,, \tag{2}$$

where σ is the stress vector in the element and $\delta\varepsilon$ is the virtual strain vector due to $\delta\mathbf{u}$.

If the strain in the element is interpolated in terms of nodal displacement by:

$$\varepsilon = \overline{\mathbf{B}}\ \mathbf{U}^{(e)}, \tag{3}$$

then, equation (2) can be rewritten as:

$$\delta \mathbf{W}_e^{\text{int}} = \delta \mathbf{U}^{(e)\,t} \int_{V_e} \overline{\mathbf{B}}^t \sigma \, \mathrm{d}V, \tag{4}$$

where $\overline{\mathbf{B}}$ is the gradient matrix.

3 ONE-POINT QUADRATURE EIGHT-NODE HEXAHEDRAL ELEMENT WITH HOURGLASS CONTROL

For an eight-node hexahedral element, the spatial coordinates, x_i, and the displacement components, u_i, in the element are approximated in terms of nodal values, x_{ia} and u_{ia}, by:

$$x_i = \sum_{a=1}^{8} N_a x_{ia}\ , \tag{5}$$

$$u_i = \sum_{a=1}^{8} N_a u_{ia}\ , \tag{6}$$

where the trilinear shape functions are expressed as:

$$N_a(\xi,\eta,\zeta) = \frac{1}{8}(1+\xi_a\xi)(1+\eta_a\eta)(1+\zeta_a\zeta), \tag{7}$$

and the subscript i denotes coordinate components (x, y, z) ranging from one to three and a denotes the element nodal numbers ranging from one to eight. The referential coordinates ξ, η e ζ of node a are denoted by ξ_a, η_a e ζ_a, respectively.

If the following column vectors are defined for nodal coordinates in the spatial system and the natural system:

$$\mathbf{x}_1^t = \mathbf{x}^t = [x_1, x_2, x_3, x_4, x_5, x_6, x_7, x_8], \tag{8}$$

$$\mathbf{x}_2^t = \mathbf{y}^t = [y_1, y_2, y_3, y_4, y_5, y_6, y_7, y_8], \tag{9}$$

$$\mathbf{x}_3^t = \mathbf{z}^t = [z_1, z_2, z_3, z_4, z_5, z_6, z_7, z_8], \tag{10}$$

$$\xi^t = [-1,+1,+1,-1,-1,+1,+1,-1], \tag{11}$$

$$\eta^t = [-1,-1,+1,+1,-1,-1,+1,+1], \tag{12}$$

$$\zeta^t = [-1,-1,-1,-1,+1,+1,+1,+1], \tag{13}$$

the Jacobian matrix at the center of the element ($\xi = \eta = \zeta = 0$) can be evaluated as [8]:

$$\mathbf{J}(0) = \frac{1}{8}\begin{bmatrix} \xi^t\mathbf{x} & \xi^t\mathbf{y} & \xi^t\mathbf{z} \\ \eta^t\mathbf{x} & \eta^t\mathbf{y} & \eta^t\mathbf{z} \\ \zeta^t\mathbf{x} & \zeta^t\mathbf{y} & \zeta^t\mathbf{z} \end{bmatrix}, \tag{14}$$

and its determinant j_o can be written as:

$$j_o = \det|\mathbf{J}(\mathbf{0})| = \frac{1}{512}\begin{vmatrix} \xi^t\mathbf{x} & \xi^t\mathbf{y} & \xi^t\mathbf{z} \\ \eta^t\mathbf{x} & \eta^t\mathbf{y} & \eta^t\mathbf{z} \\ \zeta^t\mathbf{x} & \zeta^t\mathbf{y} & \zeta^t\mathbf{z} \end{vmatrix} = \frac{1}{8}V_e, \tag{15}$$

where V_e is the volume of the 8-node hexahedral element.

To identify the deformation modes of the element [6], the gradient submatrices $\mathbf{B}_a(0)$ at the center of the element are defined as follows:

$$\mathbf{B}_a(0) = \begin{bmatrix} \dfrac{\partial \mathbf{N}_a(0)}{\partial x} \\ \dfrac{\partial \mathbf{N}_a(0)}{\partial y} \\ \dfrac{\partial \mathbf{N}_a(0)}{\partial z} \end{bmatrix} = \begin{bmatrix} \mathbf{b}_1 \\ \mathbf{b}_2 \\ \mathbf{b}_3 \end{bmatrix}, \ (a = 1,2,...,8), \tag{16}$$

If the inverse matrix of $\mathbf{J}(0)$ is denoted by $\mathbf{D}$, then the gradient vectors $\mathbf{b}_1$, $\mathbf{b}_2$ and $\mathbf{b}_3$ in equation (16) can be shown to be [8]:

$$\mathbf{b}_1 = \{b_{1a}\} = \frac{1}{8}\left[D_{11}\xi + D_{12}\eta + D_{13}\zeta\right], \tag{17}$$

$$\mathbf{b}_2 = \{b_{2a}\} = \frac{1}{8}\left[D_{21}\xi + D_{22}\eta + D_{23}\zeta\right], \tag{18}$$

$$\mathbf{b}_3 = \{b_{3a}\} = \frac{1}{8}\left[D_{31}\xi + D_{32}\eta + D_{33}\zeta\right]. \tag{19}$$

To alleviate volumetric locking, the idea underlying reduced-selective integration [9] is used. The gradient matrix is decomposed into two parts [7]:

$$\overline{\mathbf{B}}(\xi,\eta,\zeta) = \widetilde{\mathbf{B}}(\mathbf{0}) + \hat{\mathbf{B}}(\xi,\eta,\zeta), \tag{20}$$

where $\tilde{\mathbf{B}}(\mathbf{0})$ is the gradient matrix corresponding to the dilatational part of strain vector, evaluated at the element center only, and $\hat{\mathbf{B}}(\xi,\eta,\zeta)$ is the gradient matrix corresponding to the deviatoric part of the strain vector.

Then, equation (4) can be rewritten as:

$$\delta \mathbf{W}_e^{\text{int}} = \delta \mathbf{U}^{(e)t} \int_{V_e} [\tilde{\mathbf{B}}^t(\mathbf{0}) + \hat{\mathbf{B}}^t(\xi,\eta,\zeta)]\, \sigma(\xi,\eta,\zeta)\, dV \,. \tag{21}$$

Expanding $\hat{\mathbf{B}}(\xi,\eta,\zeta)$ in a Taylor series at the element center up to bilinear terms, equation (20) can be rewritten as:

$$\begin{aligned} \overline{\mathbf{B}}(\xi,\eta,\zeta) = \mathbf{B}(\mathbf{0}) + \hat{\mathbf{B}}_{,\xi}(\mathbf{0})\xi + \hat{\mathbf{B}}_{,\eta}(\mathbf{0})\eta + \hat{\mathbf{B}}_{,\zeta}(\mathbf{0})\zeta + \\ 2\hat{\mathbf{B}}_{,\xi\eta}(\mathbf{0})\xi\eta + 2\hat{\mathbf{B}}_{,\eta\zeta}(\mathbf{0})\eta\zeta + 2\hat{\mathbf{B}}_{,\xi\zeta}(\mathbf{0})\xi\zeta \,, \end{aligned} \tag{22}$$

where $\mathbf{B}(0)$ is the one-point quadrature gradient matrix contributed from both the dilatational and deviatoric parts:

$$\mathbf{B}(\mathbf{0}) = \tilde{\mathbf{B}}(\mathbf{0}) + \hat{\mathbf{B}}(\mathbf{0}). \tag{23}$$

The other terms on the right-hand side of equation (22) are the gradient matrices corresponding to non-constant deviatoric strain. The first and second derivatives of $\overline{\mathbf{B}}$ are obtained after some tedious algebra and can be found in *Liu et al.*[8].

The stress vector is also expanded in a Taylor series about the element center up to bilinear terms:

$$\begin{aligned} \sigma(\xi,\eta,\zeta) = \sigma(\mathbf{0}) + \hat{\sigma}_{,\xi}(\mathbf{0})\xi + \hat{\sigma}_{,\eta}(\mathbf{0})\eta + \hat{\sigma}_{,\zeta}(\mathbf{0})\zeta + \\ 2\hat{\sigma}_{,\xi\eta}(\mathbf{0})\xi\eta + 2\hat{\sigma}_{,\eta\zeta}(\mathbf{0})\eta\zeta + 2\hat{\sigma}_{,\xi\zeta}(\mathbf{0})\xi\zeta \,. \end{aligned} \tag{24}$$

By substituting equation (22) and (24) into equation (21), we can integrate and obtain the internal virtual work of the element as:

$$\begin{aligned} \delta \mathbf{W}_e^{\text{int}} = \delta \mathbf{U}^{(e)t} \Big[\mathbf{B}^t(\mathbf{0})\sigma(\mathbf{0}) + \frac{1}{3}\hat{\mathbf{B}}_{,\xi}^t(\mathbf{0})\hat{\sigma}_{,\xi}(\mathbf{0}) + \frac{1}{3}\hat{\mathbf{B}}_{,\eta}^t(\mathbf{0})\hat{\sigma}_{,\eta}(\mathbf{0}) + \frac{1}{3}\hat{\mathbf{B}}_{,\zeta}^t(\mathbf{0})\hat{\sigma}_{,\zeta}(\mathbf{0}) + \\ \frac{1}{9}\hat{\mathbf{B}}_{,\xi\eta}^t(\mathbf{0})\hat{\sigma}_{,\xi\eta}(\mathbf{0}) + \frac{1}{9}\hat{\mathbf{B}}_{,\eta\zeta}^t(\mathbf{0})\hat{\sigma}_{,\eta\zeta}(\mathbf{0}) + \frac{1}{9}\hat{\mathbf{B}}_{,\xi\zeta}^t(\mathbf{0})\hat{\sigma}_{,\xi\zeta}(\mathbf{0}) \Big] V_e \,, \end{aligned} \tag{25}$$

where the first term on the right-hand side of equation (25) is the one-point quadrature internal virtual work. The other terms are also evaluated at the element center to provide the

stabilization of the element [7].

By assuming that the Jacobian is a constant, 1/8 of the element volume, the one-point quadrature element internal force vector without hourglass control can be expressed by:

$$\mathbf{f}^{e} = \mathbf{B}^{t}(\mathbf{0})\,\sigma(\mathbf{0})\,V_{e}. \tag{26}$$

The element stiffness matrix for the underintegrated element can be obtained by using the stress-strain law $\sigma = \mathbf{C}\varepsilon$ in conjunction with $\varepsilon = \mathbf{B}\,\mathbf{U}$:

$$\mathbf{f}^{e} = \mathbf{K}^{e}\,\mathbf{U}, \tag{27}$$

where $\mathbf{K}^{e}$ is the element stiffness matrix evaluated at the element center without hourglass control and it is given by:

$$\mathbf{K}^{e} = \mathbf{B}^{t}(\mathbf{0})\,\mathbf{C}\,\mathbf{B}(\mathbf{0})\,V_{e}, \tag{28}$$

which is rank insufficiency and may exhibit spurious singular modes. To eliminate these spurious singular modes, it is necessary to add the hourglass-resisting force, $\mathbf{f}^{hg}$, to the element internal force vector as:

$$\mathbf{f}^{\text{int}} = \mathbf{f}^{e} + \mathbf{f}^{hg}. \tag{29}$$

By observing equations (25), (26) and (29), $\mathbf{f}^{hg}$ may be defined as:

$$\begin{aligned}\mathbf{f}^{hg} = \Bigg[& \frac{1}{3}\hat{\mathbf{B}}^{t}_{,\xi}(\mathbf{0})\,\hat{\sigma}_{,\xi}(\mathbf{0}) + \frac{1}{3}\hat{\mathbf{B}}^{t}_{,\eta}(\mathbf{0})\,\hat{\sigma}_{,\eta}(\mathbf{0}) + \frac{1}{3}\hat{\mathbf{B}}^{t}_{,\zeta}(\mathbf{0})\,\hat{\sigma}_{,\zeta}(\mathbf{0}) + \\ & \frac{1}{9}\hat{\mathbf{B}}^{t}_{,\xi\eta}(\mathbf{0})\,\hat{\sigma}_{,\xi\eta}(\mathbf{0}) + \frac{1}{9}\hat{\mathbf{B}}^{t}_{,\eta\zeta}(\mathbf{0})\,\hat{\sigma}_{,\eta\zeta}(\mathbf{0}) + \frac{1}{9}\hat{\mathbf{B}}^{t}_{,\xi\zeta}(\mathbf{0})\,\hat{\sigma}_{,\xi\zeta}(\mathbf{0}) \Bigg] V_{e}.\end{aligned} \tag{30}$$

If the first and second derivatives of the stress vector can be derived from the material constitutive equations, the element stabilization stiffness matrix $\mathbf{K}^{stab}$ may be also defined as:

$$\mathbf{f}^{hg} = \mathbf{K}^{stab}\,\mathbf{U}. \tag{31}$$

This matrix is added to the element stiffness matrix, $\mathbf{K}^{e}$, so the element stiffness matrix $\mathbf{K}$ is rank sufficient and is given by:

$$\mathbf{K} = \mathbf{K}^{e} + \mathbf{K}^{stab}. \tag{32}$$

To avoid the derivation of the relationships between the first and second derivative of the stress vector and the nodal displacement vector in equation (30), Hu and Nagy [7] proposed a "stabilization matrix", **E**, to satisfy following constitutive relations:

$$\begin{aligned} \hat{\sigma}_{,\xi} &= \mathbf{E}\,\hat{\varepsilon}_{,\xi}\ , \quad \hat{\sigma}_{,\eta} = \mathbf{E}\,\hat{\varepsilon}_{,\eta}\ , \quad \hat{\sigma}_{,\zeta} = \mathbf{E}\,\hat{\varepsilon}_{,\zeta}\ , \\ \hat{\sigma}_{,\xi\eta} &= \mathbf{E}\,\hat{\varepsilon}_{,\xi\eta}\ , \quad \hat{\sigma}_{,\eta\zeta} = \mathbf{E}\,\hat{\varepsilon}_{,\eta\zeta}\ , \quad \hat{\sigma}_{,\xi\zeta} = \mathbf{E}\,\hat{\varepsilon}_{,\xi\zeta}\ . \end{aligned} \tag{33}$$

where **E** is the elastic material modulus matrix, which is the simplest form for computation and is given as:

$$\mathbf{E}_{6x6} = \begin{bmatrix} \mathbf{e}_{3x3} & \mathbf{0} \\ \mathbf{0} & \mathbf{e}_{3x3} \end{bmatrix}, \tag{34}$$

where,

$$\mathbf{e} = \begin{bmatrix} 2\mu & 0 & 0 \\ 0 & 2\mu & 0 \\ 0 & 0 & 2\mu \end{bmatrix}, \tag{35}$$

and μ is the Lame constant.

Then, by substituting equations (33) in (30), the element stabilization stiffness matrix is obtained in the following form:

$$\begin{aligned} \mathbf{K}^{stab} = \Bigg[& \frac{1}{3}\hat{\mathbf{B}}^t_{,\xi}(\mathbf{0})\,\mathbf{E}\,\hat{\mathbf{B}}^t_{,\xi}(\mathbf{0}) + \frac{1}{3}\hat{\mathbf{B}}^t_{,\eta}(\mathbf{0})\,\mathbf{E}\,\hat{\mathbf{B}}^t_{,\eta}(\mathbf{0}) + \frac{1}{3}\hat{\mathbf{B}}^t_{,\zeta}(\mathbf{0})\,\mathbf{E}\,\hat{\mathbf{B}}^t_{,\zeta}(\mathbf{0}) + \\ & \frac{1}{9}\hat{\mathbf{B}}^t_{,\xi\eta}(\mathbf{0})\,\mathbf{E}\,\hat{\mathbf{B}}^t_{,\xi\eta}(\mathbf{0}) + \frac{1}{9}\hat{\mathbf{B}}^t_{,\eta\zeta}(\mathbf{0})\,\mathbf{E}\,\hat{\mathbf{B}}^t_{,\eta\zeta}(\mathbf{0}) + \frac{1}{9}\hat{\mathbf{B}}^t_{,\xi\zeta}(\mathbf{0})\,\mathbf{E}\,\hat{\mathbf{B}}^t_{,\xi\zeta}(\mathbf{0}) \Bigg] V_e\,. \end{aligned} \tag{36}$$

The element developed so far is free of volumetric locking and has no spurious singular modes. However, it is not suitable to plate/shell analysis owing to the shear and membrane locking in thin structures and it cannot pass the patch test if the mesh is irregular.

To remove shear locking, the gradient submatrices corresponding to the assume shear strain is written in an orthogonal corotational coordinate system rotating with the element and each shear-strain component is linearly interpolated in one referential coordinate direction only [7]:

$$\varepsilon_{xy}(\xi,\eta,\zeta) = \varepsilon_{xy}(\mathbf{0}) + \hat{\varepsilon}_{xy,\zeta}(\mathbf{0})\zeta\ , \tag{37}$$

$$\varepsilon_{yz}(\xi,\eta,\zeta) = \varepsilon_{yz}(\mathbf{0}) + \hat{\varepsilon}_{yz,\xi}(\mathbf{0})\xi\ , \tag{38}$$

$$\varepsilon_{xz}(\xi,\eta,\zeta) = \varepsilon_{xz}(\mathbf{0}) + \hat{\varepsilon}_{xz,\eta}(\mathbf{0})\eta\,, \tag{39}$$

which imply:

$$\hat{\mathbf{B}}_{xy,\xi}(\mathbf{0}) = \hat{\mathbf{B}}_{xy,\eta}(\mathbf{0}) = \hat{\mathbf{B}}_{xy,\xi\eta}(\mathbf{0}) = \hat{\mathbf{B}}_{xy,\eta\zeta}(\mathbf{0}) = \hat{\mathbf{B}}_{xy,\xi\zeta}(\mathbf{0}) = \mathbf{0}\,, \tag{40}$$

$$\hat{\mathbf{B}}_{yz,\eta}(\mathbf{0}) = \hat{\mathbf{B}}_{yz,\zeta}(\mathbf{0}) = \hat{\mathbf{B}}_{yz,\xi\eta}(\mathbf{0}) = \hat{\mathbf{B}}_{yz,\eta\zeta}(\mathbf{0}) = \hat{\mathbf{B}}_{yz,\xi\zeta}(\mathbf{0}) = \mathbf{0}\,, \tag{41}$$

$$\hat{\mathbf{B}}_{xz,\xi}(\mathbf{0}) = \hat{\mathbf{B}}_{xz,\zeta}(\mathbf{0}) = \hat{\mathbf{B}}_{xz,\xi\eta}(\mathbf{0}) = \hat{\mathbf{B}}_{xz,\eta\zeta}(\mathbf{0}) = \hat{\mathbf{B}}_{xz,\xi\zeta}(\mathbf{0}) = \mathbf{0}\,, \tag{42}$$

where $\hat{\mathbf{B}}_{xy}$, $\hat{\mathbf{B}}_{yz}$ e $\hat{\mathbf{B}}_{xz}$ are the gradient matrices corresponding to the deviatoric strain components $\hat{\varepsilon}_{xy}$, $\hat{\varepsilon}_{yz}$ e $\hat{\varepsilon}_{xz}$, respectively.

The one-point quadrature element will pass in the patch test when it is skewed if the gradient matrix $\mathbf{B}_a(0)$ is replaced by the uniform gradient $\mathbf{B'}_a(0)$ defined by Flanagan and Belytschko [2] as:

$$\mathbf{B'}_a = \frac{1}{V_e}\int_{V_e}\mathbf{B}_a(\xi,\eta,\zeta)\,dV\,. \tag{43}$$

4 CORROTATIONAL APPROACH FOR GEOMETRICALLY NONLINEAR ANALYSIS

It has been shown that the elimination of the shear locking depends on the proper treatment of the shear strain. In order to avoid this effect, it is necessary to attach a local coordinate system to the element so that the corotational system described in Liu *et al*.[8] is employed.

Theoretically, the motion of a continuous medium can always be decomposed into a rigid body motion followed by a pure deformation. If the finite element discretization is fine enough to provide a valid approximation of the continuum, this decomposition can be performed at the element level. If the rigid body motion is eliminated from the total displacement field which corresponds to large displacements and rotation but small strains, the pure deformation part is always a small quantity relative to the element dimensions [9].

4.1 Corotational stress updates

For stress and strain updates, we assume that all variables at the previous load step t_n are known. Then, it is only necessary to calculate the strain increment from the displacement field within the load increment $[t_n, t_{n+1}]$, and the procedure described by Liu *et al*.[8] to calculate the deformation part ($\Delta\hat{\mathbf{u}}^{\text{def}}$) of the displacement increment in a corotational system is used. In this work, $\Delta\hat{\mathbf{u}}^{\text{def}}$ is referred to the mid-point configuration ($t_{n+1/2}$).

Denoting the spatial coordinates of the configuration, Ω_n, and the current configuration,

Ω_{n+1}, as $\boldsymbol{x}_n$ e $\boldsymbol{x}_{n+1}$ in the fixed global Cartesian coordinate system Ox, as shown in Fig. 1, the coordinates in the corresponding corotational Cartesian coordinate system, $O\hat{x}_n$ e $O\hat{x}_{n+1}$, can be obtained by the following transformation rules:

$$\hat{\mathbf{x}}_n = \mathbf{R}_n \mathbf{x}_n , \tag{44}$$

$$\hat{\mathbf{x}}_{n+1} = \mathbf{R}_{n+1} \mathbf{x}_{n+1} , \tag{45}$$

where $\mathbf{R}_n$ e $\mathbf{R}_{n+1}$ are the orthogonal transformation matrices which rotates the global coordinate system to the corresponding corotational coordinate system, respectively (defined in Liu *et al.*[8]).

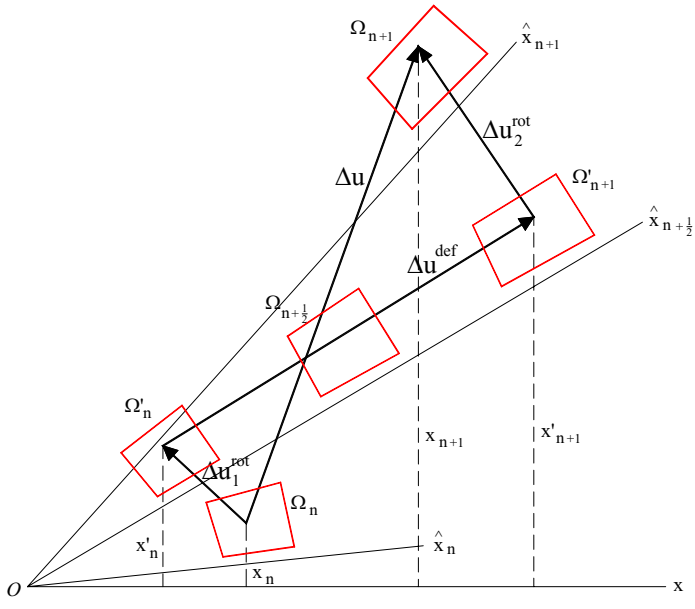

Figure 1: Separation of the displacement increment. Liu *et al.*[8].

Since the strain increment is referred to the configuration at $t = t_{n+1/2}$, assuming the velocities within the increment $[t_n, t_{n+1}]$ are constant, it is obtained:

$$\mathbf{x}_{n+1/2} = \frac{1}{2}\left(\mathbf{x}_n + \mathbf{x}_{n+1}\right), \tag{46}$$

$$\hat{\mathbf{x}}_{n+1/2} = \mathbf{R}_{n+1/2} \mathbf{x}_{n+1/2} . \tag{47}$$

Similar to polar decomposition, an incremental deformation can be separated into the summation of the pure deformation and the pure rotation [8]. Letting $\Delta\mathbf{u}$ indicate the displacement increment within the load increment $[t_n, t_{n+1}]$, it may be written:

$$\Delta\mathbf{u} = \Delta\mathbf{u}^{\text{def}} + \Delta\mathbf{u}^{\text{rot}}, \tag{48}$$

where $\Delta\mathbf{u}^{\text{def}}$ e $\Delta\mathbf{u}^{\text{rot}}$ are, respectively, the deformation part and the pure rotation part of the displacement increment in the global coordinate system.

In order to obtain the deformation part of the displacement increment referred to the configuration at $t = t_{n+1/2}$, it is necessary to find the rigid rotation from Ω_n to Ω_{n+1}. Defining two virtual configurations, Ω'_n and Ω'_{n+1}, by rotating the element bodies Ω_n and Ω_{n+1} into the corotational system $O\hat{x}_{n+1/2}$ (Fig. 1) and denoting $\hat{\mathbf{x}}'_n$ and $\hat{\mathbf{x}}'_{n+1}$ as the coordinates of Ω'_n and Ω'_{n+1} in the corotational system $O\hat{x}_{n+1/2}$,it is obtained:

$$\hat{\mathbf{x}}'_n = \hat{\mathbf{x}}_n, \qquad \hat{\mathbf{x}}'_{n+1} = \hat{\mathbf{x}}_{n+1}. \tag{49}$$

It may be seen that from Ω_n to Ω'_n and from Ω'_{n+1} to Ω_{n+1} the body experiences two rigid rotations and the rotation displacement are given by [8]:

$$\Delta\mathbf{u}_1^{\text{rot}} = \mathbf{x}'_n - \mathbf{x}_n = \mathbf{R}^t_{n+1/2}\hat{\mathbf{x}}'_n - \mathbf{x}_n = \mathbf{R}^t_{n+1/2}\hat{\mathbf{x}}_n - \mathbf{x}_n, \tag{50}$$

$$\Delta\mathbf{u}_2^{\text{rot}} = \mathbf{x}_{n+1} - \mathbf{x}'_{n+1} = \mathbf{x}_{n+1} - \mathbf{R}^t_{n+1/2}\hat{\mathbf{x}}'_{n+1} = \mathbf{x}_{n+1} - \mathbf{R}^t_{n+1/2}\hat{\mathbf{x}}_{n+1}. \tag{51}$$

Thus, the total rotation displacement increment can be expressed as:

$$\Delta\mathbf{u}^{\text{rot}} = \Delta\mathbf{u}_1^{\text{rot}} + \Delta\mathbf{u}_2^{\text{rot}} = \mathbf{x}_{n+1} - \mathbf{x}_n - \mathbf{R}^t_{n+1/2}\left(\hat{\mathbf{x}}_{n+1} - \hat{\mathbf{x}}_n\right) = \Delta\mathbf{u} - \mathbf{R}^t_{n+1/2}\left(\hat{\mathbf{x}}_{n+1} - \hat{\mathbf{x}}_n\right). \tag{52}$$

Then, the deformation part of the displacement increment referred to $\Omega_{n+1/2}$ is:

$$\Delta\mathbf{u}^{\text{def}} = \Delta\mathbf{u} - \Delta\mathbf{u}^{\text{rot}} = \mathbf{R}^t_{n+1/2}\left(\hat{\mathbf{x}}_{n+1} - \hat{\mathbf{x}}_n\right). \tag{53}$$

Therefore, the deformation displacement increment in the corotational system $O\hat{x}_{n+1/2}$ is obtained as:

$$\Delta\hat{\mathbf{u}}^{\text{def}} = \mathbf{R}_{n+1/2}\Delta\mathbf{u}^{\text{def}} = \hat{\mathbf{x}}_{n+1} - \hat{\mathbf{x}}_n. \tag{54}$$

Since the corotational coordinate system rotates with the configuration, it is used the corotational Cauchy stress, which is objective, as stress measure. The rate of deformation (or velocity strain vector), $\dot{\varepsilon}$, also defined in the corotational coordinate system, is used as the

measure of the strain rate [8]:

$$\dot{\varepsilon} = \hat{\mathbf{d}} = \frac{1}{2}\left[\frac{\partial \hat{\mathbf{v}}^{\text{def}}}{\partial \hat{\mathbf{x}}} + \left(\frac{\partial \hat{\mathbf{v}}^{\text{def}}}{\partial \hat{\mathbf{x}}}\right)^{t}\right], \tag{55}$$

where $\hat{\mathbf{v}}^{\text{def}}$ is the deformation part of the velocity in the corotational system $\hat{x}$.

Then, the strain increment is given by the mid-point integration of the velocity strain tensor,

$$\Delta\hat{\varepsilon} = \int_{t_n}^{t_{n+1}} \hat{\mathbf{d}}\, d\tau \doteq \frac{1}{2}\left[\frac{\partial \Delta\hat{\mathbf{u}}^{\text{def}}}{\partial \hat{\mathbf{x}}_{n+1/2}} + \left(\frac{\partial \Delta\hat{\mathbf{u}}^{\text{def}}}{\partial \hat{\mathbf{x}}_{n+1/2}}\right)^{t}\right]. \tag{56}$$

4.2 Constitutive equation

As the material rate for the Cauchy stress tensor is not a frame-invariant rate, it is employed the Green-Naghdi objective rate, which gives the following material tangent matrix [8]:

$$\mathbf{T}(\sigma) = \begin{bmatrix} \mathbf{C}_{6x6} & \mathbf{0}_{6x3} \\ \mathbf{0}_{3x6} & \mathbf{0}_{3x3} \end{bmatrix} + \hat{\mathbf{T}}(\sigma), \tag{57}$$

where $\mathbf{0}_{m\times n}$ denotes the $m\times n$ zero matrix, $\mathbf{C}$ is a 6×6 matrix of material tangent moduli and $\hat{\mathbf{T}}(\sigma)$, the initial-stress matrix, is defined below:

$$\hat{\mathbf{T}}(\sigma) = \begin{bmatrix}
2\sigma_{11} & 0 & 0 & \sigma_{12} & 0 & \sigma_{13} & \sigma_{12} & 0 & -\sigma_{13} \\
 & 2\sigma_{22} & 0 & \sigma_{12} & \sigma_{23} & 0 & -\sigma_{12} & \sigma_{23} & 0 \\
 & & 2\sigma_{33} & 0 & \sigma_{23} & \sigma_{13} & 0 & -\sigma_{23} & \sigma_{13} \\
 & & & \frac{\sigma_{11}+\sigma_{22}}{2} & \frac{\sigma_{13}}{2} & \frac{\sigma_{23}}{2} & \frac{\sigma_{22}-\sigma_{11}}{2} & \frac{\sigma_{13}}{2} & -\frac{\sigma_{23}}{2} \\
 & & & & \frac{\sigma_{22}+\sigma_{33}}{2} & \frac{\sigma_{12}}{2} & -\frac{\sigma_{13}}{2} & \frac{\sigma_{33}-\sigma_{22}}{2} & \frac{\sigma_{12}}{2} \\
 & & & & & \frac{\sigma_{33}+\sigma_{11}}{2} & \frac{\sigma_{23}}{2} & -\frac{\sigma_{12}}{2} & \frac{\sigma_{11}-\sigma_{33}}{2} \\
 & & \text{symm.} & & & & \frac{\sigma_{11}+\sigma_{22}}{2} & -\frac{\sigma_{13}}{2} & -\frac{\sigma_{23}}{2} \\
 & & & & & & & \frac{\sigma_{22}+\sigma_{33}}{2} & -\frac{\sigma_{12}}{2} \\
 & & & & & & & & \frac{\sigma_{33}+\sigma_{11}}{2}
\end{bmatrix} \tag{58}$$

The $\mathbf{T}(\sigma)$ matrix is arranged to be compatible with the following ordering of strain and rotation components:

$$\varepsilon^t = \left[\dot{\varepsilon}_{11}\ \dot{\varepsilon}_{22}\ \dot{\varepsilon}_{33}\ \dot{\varepsilon}_{12}\ \dot{\varepsilon}_{23}\ \dot{\varepsilon}_{31}\ \dot{\omega}_{12}\ \dot{\omega}_{23}\ \dot{\omega}_{31}\right]. \tag{59}$$

Then, the equilibrium equation at *j*th iteration can be written in the corotational coordinate system as:

$$\hat{\mathbf{K}}_{j-1}\,\Delta\hat{\mathbf{U}} = \hat{\mathbf{P}}_j - \hat{\mathbf{f}}_{j-1}, \tag{60}$$

where the $\Delta\hat{\mathbf{U}}$ is the displacement increment vector; $\hat{\mathbf{P}}_j$ is the externally applied nodal point forces and the tangent stiffness matrix $\hat{\mathbf{K}}_{j-1}$ and the internal nodal force vector $\hat{\mathbf{f}}_{j-1}$ are:

$$\hat{\mathbf{K}}_{j-1} = \mathbf{B}'^t(\mathbf{0})\left(\mathbf{C} + \hat{\mathbf{T}}_{j-1}\right)\mathbf{B}'(\mathbf{0}) + \mathbf{K}^{stab}, \tag{61}$$

$$\hat{\mathbf{f}}_{j-1} = \mathbf{f}^e + \mathbf{f}^{hg}. \tag{62}$$

The tangent stiffness and nodal forces are transformed into the global coordinate system as:

$$\mathbf{K}_j = \mathbf{R}_j^t \hat{\mathbf{K}}_j \mathbf{R}_j, \tag{63}$$

$$\mathbf{r}_j = \hat{\mathbf{P}}_j - \hat{\mathbf{f}}_{j-1} = \mathbf{R}_j^t\,\hat{\mathbf{r}}_j, \tag{64}$$

where $\mathbf{R}$ is the transformation matrix of the corotational system defined by Liu et al.[8].

5 NUMERICAL EXAMPLES

Numerical examples, exhibiting highly nonlinear behavior, are presented to test and verify the element included in this work for geometrically nonlinear analysis. The post-buckling performance of thin shells using the one-point quadrature eight-node brick element is compared to reported results in the literature with different types of shell elements. The efficiency of this element to handle with nearly-incompressible materials and to solve linear static and dynamic problems has already been demonstrated in others publication [7, 13].

In order to obtain the post-buckling response, the Generalized Displacement Control Method [14] was implemented.

5.1 Buckling of a deep circular arch

In this example, the pre and post-buckling response of a clamped-clamped circular arch under a concentrated mid-span load is considered, as shown in Fig. 2. Due to symmetry, only half of the arch was discretized into a mesh of 40×4×1 (length×height×width) three-

dimensional elements. The load-deflection curve, corresponding to the mid-span point, is presented in Fig. 3. It may be observed that the result is very close to that published by Jiang and Chernuka [9], where 20 shell elements were employed. The deformed configurations of the arch are displayed in Fig. 4.

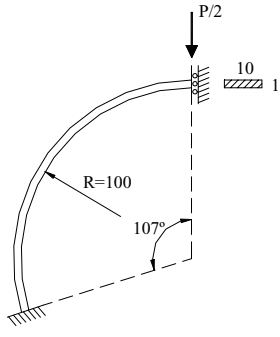

Figure 2: Half of the circular arch under a concentrated mid-span load. E =1,2×10^4; ν = 0,3.

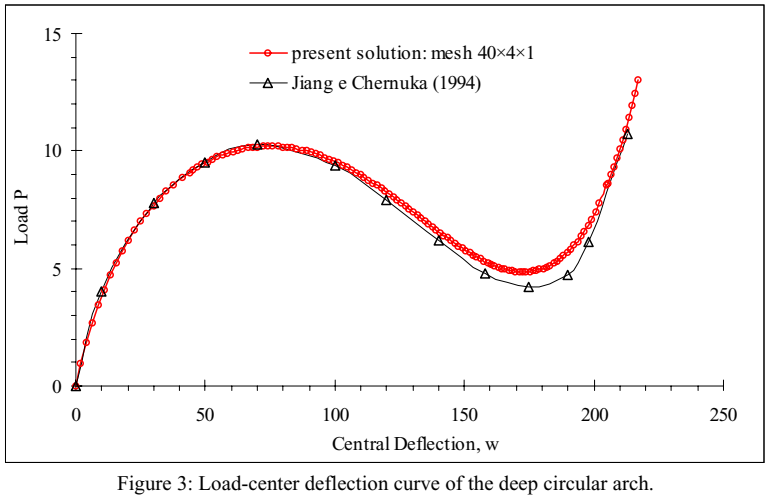

Figure 3: Load-center deflection curve of the deep circular arch.

5.2 Snap-through of a hinged shallow cylindrical shell

This example considers the large displacement behavior of a cylindrical panel under a concentrated vertical load, shown in Fig. 5. The curved edges of the panel are assumed to be free while the straight edges are hinged (fixed only the mid-line in the thickness).

Figure 4: Deformed configuration of the circular arch corresponding to w = 38; 78; 140.

Due to the symmetry of the problem, only one quarter of the panel was idealized into a mesh of 10×10×4 hexahedral elements (4 elements were used in the thickness direction). The load-center deflection curves is presented in Fig. 6. The results agree very well with the curve presented by Jiang and Chernuka [9]. In this paper, Jiang and Chernuka used a mesh of 6×6 shell elements.

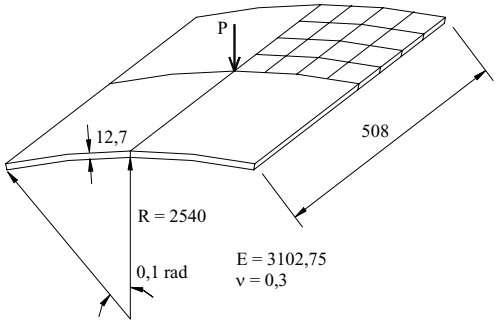

Figure 5: Cylindrical shell.

5.3 Cantilever beam with a concentrated end moment

The cantilever beam subjected to a pair of follower concentrated loads applied at the free end is considered in this example, as shown in Fig. 7. Under these loads, it is possible to represent a concentrated end moment at the free end and solve this classical elastic problem used as a benchmark problem for large deformation analysis using shell/plate elements. The beam was discretized into a mesh of 40×4×1 (length×height×width) hexahedral elements. The moment-deflection curves given in Fig. 8 show that an excellent agreement with the results published by Shi and Voyiadjis [10] was obtained. Shi and Voyiadjis used 10 plate elements. Fig. 9 depicts several deformed configuration during load.

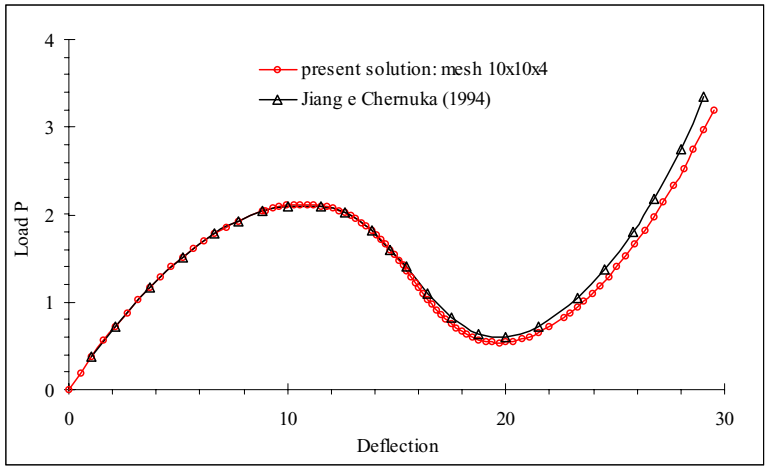

Figure 6: Load-deflection curve of the cylindrical shell.

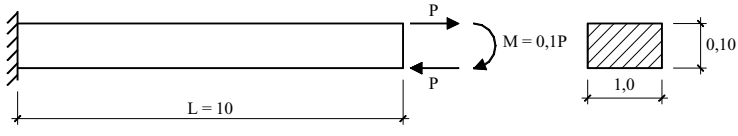

Figure 7: Cantilever beam with a concentrated end moment. $E=1{,}2\times10^5$, $\nu=0{,}0$.

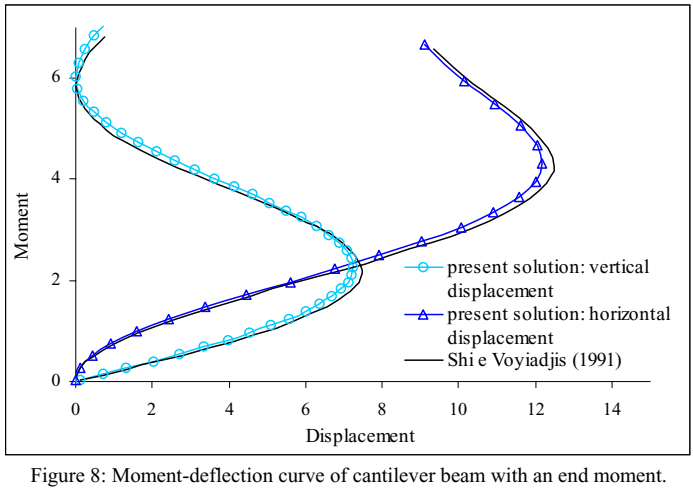

Figure 8: Moment-deflection curve of cantilever beam with an end moment.

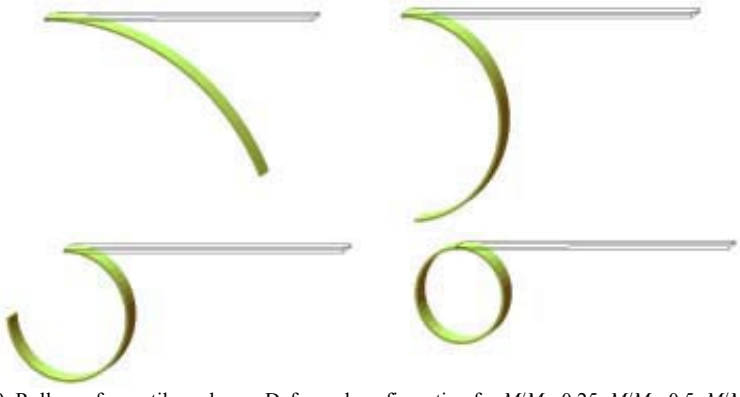

Figure 9: Roll-up of a cantilever beam. Deformed configuration for M/M_o=0,25; M/M_o=0,5; M/M_o=0,75; M/M_o=1,00.

6 CONCLUSIONS

A one-point quadrature eight-node hexahedral element with hourglass control was successfully implemented for geometrically nonlinear analysis with arbitrarily large displacement and rotation. The effectiveness and robustness of this element have been demonstrated through numerical examples. Future works will include dynamic nonlinear analysis, as well as physical nonlinearities.

7 ACKNOLEDGEMENTS

The authors wish to thank CAPES and CNPQ for their support.

8 REFERENCES

[1] T. Belytschko, W. K. Liu and M. Moran, *Nonlinear finite elements for continua and strucutures*, Wiley, (2001).

[2] D. P. Flanagan and T. Belytschko, "A uniform strain hexahedron and quadrilateral with orthogonal hourglass control", *Int. J. Num. Meth. Engng.*, **17**, 679-706 (1983).

[3] T. Belytschko, J. S.-J. Ong, W. K. Liu and J. M. Kennedy, "Hourglass control in linear and nonlinear problems", *Comput. Methods Appl. Mech. Eng.*, **43**, 251-276 (1984).

[4] W. K. Liu, J. S.-J. Ong and R. A. Uras, "Finite element stabilization matrices – a unification approach", *Comput. Methods Appl. Mech. Eng.*, **53**, 13-46 (1985).

[5] J. C. Schulz, "Finite element hourglassing control", *Int. J. Num. Meth. Engng.*, **21**, 1039-1048 (1985).

[6] W. K. Liu, Y.-K. Hu and T. Belytschko, "Multiple quadrature underintegrated finite elements", *Int. J. Num. Meth. Engng.*, **37**, 3263-3289 (1994).

[7] Y.-K. Hu and L. I. Nagy, "A one-point quadrature eight-node brick element with hourglass control", *Computer & Structure*, **65**, 893-902 (1997).
[8] W. K. Liu, Y. Guo, S. Tang and T. Belytschko, "A multiple-quadrature eight-node hexahedral finite element for large deformation elastoplastic analysis", *Comput. Methods Appl. Mech. Eng.*, **154**, 69-132 (1998).
[9] L. Jiang and M. W. Chernuka, "A simple four-node corotational shell element for arbitrarily large rotation", *Computers & Structure*, **53**, 1123-1132 (1994).
[10] G. Shi and G. Z. Voyiadjis, "Geometrically nonlinear analysis of plates by assumed strain elements with explicit tangent stiffness matrix", *Computers & Structure*, **41**, 757-763 (1991).
[11] Y. Zhu and Thomas Zacharia, "A new one-point quadrature, quadrilateral shell element with drilling degrees of freedom", *Comput. Methods Appl. Mech. Eng.*, **136**, 165-203 (1996).
[12] T. J. Hughes, "Generalization of selective integration procedures to anisotropic and nonlinear media", *Int. J. Num. Meth. Engng.*, **15**, 1413-1418 (1980).
[13] L. A. Duarte and A. M. Awruch, "Análise linear estática e dinâmica de placas e cascas através de elementos finitos hexaédricos com um ponto de integração", XXX *Jornadas Sul-Americanas de Engenharia Estrutural.*, (2002).
[14] Y.-B. Yang and M.S. Shieh, "Solution method for nonlinear problems with multiple critical points", *AIAA Journal*, **28**, 2110-2116 (1990).